archives
of thermodynamics
Vol. **44**(2023), No. 4, 3–21
DOI: 10.24425/ather.2023.149708

An in-house numerical code to assist in designing a small-scale red-hot air furnace

SYLWIA POLESEK-KARCZEWSKA*
DARIUSZ KARDAŚ
IZABELA WARDACH-ŚWIĘCICKA

The Szewalski Institute of Fluid Flow Machinery, Polish Academy of Sciences, Fiszera 14, 80-231 Gdańsk, Poland

Abstract The implementation of a sustainable development concept that involves an improvement of resource use efficiency, whilst maximizing the utilization of locally available biomass resources, has contributed to an increased interest in the combined heat and power systems based on externally fired gas turbines. Since the high-temperature gas/gas heat exchangers intended to heat the turbine inlet air are the key components of such systems, intensified research on exchangers of this type has been observed over the last decade. This work presents the in-house calculation code developed to analyze the heat transfer between the hot-side and cold-side streams in the small-scale red-hot air furnace of a unique design. The performed calculations, based on the assumed thermal and flow operation parameters and technical specifications, allowed to determine the required heat exchange surface area of the furnace to achieve the target outlet conditions. The calculation code allows for determining the geometry of a furnace, including its overall dimensions, number of tubes, and their bent sections in the heat exchange parts. The study of the laboratory-scale furnace performance has demonstrated its good agreement with the simulation results, thereby proving the code a reliable tool in designing.

Keywords: Red-hot air furnace; Design; Calculation methodology; Parametric characteristics; Heat exchange surface area

*Corresponding Author. Email: sylwia.polesek-karczewska@imp.gda.pl

Nomenclature

A	–	heat exchange surface area, cross-sectional area, m^2
$\bar{c}_p$	–	average specific heat, J/(kgK)
d	–	diameter, m
dT	–	temperature increment, K
dz	–	tube diameter, m
HTC	–	heat transfer coefficient
$\dot{H}$	–	mass flow enthalpy, W
k	–	overall heat transfer coefficient, W/(m^2K)
L	–	gas layer thickness, characteristic dimension, length of section, m
m	–	flame-to-chamber volume ratio
$\dot{m}$	–	mass flowrate, kg/s
N_p	–	number of tubes
Nu	–	Nusselt number
p	–	pressure, kPa
p_n	–	partial pressure, kPa
Pr	–	Prandtl number
$\dot{q}$	–	heat flux, W/m^2
$\dot{Q}$	–	thermal output, W
$\dot{Q}_{LHV}$	–	chemical energy, W
Re	–	Reynolds number
R_g	–	tube bending radius, m
T	–	temperature, K
X	–	mole fraction, mol/mol

Greek symbols

α	–	heat transfer coefficient, W/(m^2K)
δ	–	wall thickness, m
ε	–	emissivity
λ_w	–	thermal conductivity of tube material, W/(m K)
λ	–	excess air ratio
ρ	–	density, kg/m^3
σ	–	Stefan-Boltzmann constant, $= 5.678 \cdot 10^{-8}$ W/(m^2K^4)
θ	–	logarithmic mean temperature difference, K
ψ	–	degree of wall screening
ξ	–	slagging factor

Subscripts and superscripts

0	–	initial value
a	–	air
ad	–	adiabatic
com	–	combustion
conv	–	convection
corr	–	correction
err	–	limitation value/error value
dh	–	hydraulic diameter

f	–	fuel, fluid
fg	–	flue gas
fl	–	flame
g	–	gas, gaseous non-luminous part of the flame
i	–	iteration procedure index
in	–	inlet
inn	–	inner
j	–	iteration procedure index
k	–	iteration procedure index
l	–	luminous part of the flame
loss	–	loss to the surroundings
mid	–	between high- and medium-temperature sections
new	–	next step value
old	–	previous step value
out	–	outlet
ox	–	oxidizer (combustion air)
rad	–	radiation
s	–	surface
tot	–	total
w	–	combustion chamber wall
x, y, z	–	x-, y-, z-direction
xy	–	cross-section

Acronyms

CHP	–	combined heat and power
EFGT	–	externally-fired gas turbine
HT	–	high-temperature
THE	–	high-temperature heat exchanger
MT	–	medium-temperature
ORC	–	organic Rankine cycle
RHAF	–	red-hot air furnace

1 Introduction

Small-scale energy systems have gained increasing interest over the past decades owing to the emerging concept of the sustainable use of locally available renewable energy resources. Along with this, efforts have been intensified toward the development of conversion technologies that would meet the growing demands of distributed energy generation. Aiming at minimizing CO_2 emissions, while maximizing the system's efficiency, the focus has been put on the combined heat and power (CHP) technologies based on biomass of different kinds [1]. Besides the thermochemical methods, such as pyrolysis and gasification, combustion remains the basic route of biomass

conversion for energy purposes, due to the maturity of the technology of furnaces [2]. However, the combustion of biomass entails operational problems that are mainly caused by more intensive fouling and increased corrosion rates due to the presence of alkali compounds in the fuel. These problems may be reduced through adjustment of the operation parameters for the specific boiler design to provide efficient combustion [3]. The large diversity of biomass properties to be potentially utilized in small-scale CHP units is challenging in terms of technical and economic feasibility and, therefore, the research in the area of distributed energy systems requires further advances. Within the small power range of CHP systems (below 1 MWel), apart from the technologies involving Stirling and steam engines, or turbine organic Rankine cycle (ORC), these are the externally-fired gas turbine (EFGT) systems that are considered the promising solution [4,5], especially due to fuel flexibility [6]. The biomass furnace and the high-temperature heat exchangers (HTHEs), typically air-cooled, are the key components of the EFGT system, critical in terms of performance reliability, and the system's total cost. For this reason, efforts are undertaken to provide possibly highly efficient devices to preserve reduced energy consumption and investment costs that contribute to increased energy generation efficiency and lower emission levels. The constraint to be encountered in developing gas/gas HTHE technology is due to lower heat transfer coefficients of gas compared to those for liquid coolants, which is said to result in the air-side resistance exceeding 85% of the total thermal resistance [7]. One of the options is the furnace-integrated HTHEs. Such designs allow additionally to take advantage of thermal radiation, and simultaneously, to obtain smaller and more compact constructions which result in reducing manufacturing costs. In this context, one of the key issues is the reliable evaluation of the furnace exit gas temperature needed to define the basic design feature in terms of dividing the heat exchange surfaces into the irradiated and convection sections [8], thereby optimizing the furnace's dimensions and weight.

Commonly, computational fluid dynamics (CFD) has been involved in the designing and optimization of thermal devices. Owing to the possibility of reproducing the full geometry of a device and complex three-dimensional flow structures [9], this approach may provide more accurate predictions of thermal performance. But this will always be done at the expense of larger computing power demand. The computations become even more time-consuming when the radiation heat transfer has to be accounted for, which is the case with the heat exchangers operated under high-temperature

regimes and emitting/absorbing media such as a flue gas [10]. Precisely due to increased computational cost, radiation is often neglected [11], though it is important to the accurate predictions of the high-temperature units' performance. Żukowski *et al.* [12] used CFD tools for simulating heat transfer in a cross-current plate heat exchanger designed to heat the combustion air from the exhaust gas flow to burn waste organics in a fluidized bed furnace. The authors studied different geometries of the inter-plate space focusing on identifying the dead zones in the airflow. Thek *et al.* [13] performed CFD analysis in designing a biomass furnace and cylindrical tube bundle HTHE for a small-scale micro-CHP system of $\sim$ 100 kW nominal electric power based on a gas turbine. Through simulations, they obtained the optimized designs with reduced peaks in flue gas temperature and velocity in the furnace, and possibly evenly distributed flue gas inflow to HTHE. The latter has been designed as a two-duct heat exchanger to use different materials for each section. The higher quality and more expensive stainless steel (type 1.4876) was used only in the duct exposed to high temperatures. There are also other approaches proposed offering a reduction of CPU time. Recently, Wajs *et al.* [14] have developed a numerical model of a high-temperature mini-channel heat exchanger for a gas micro-CHP system and carried out the analysis of its thermo-hydraulic performance using OpenFOAM environment.

The relatively simple and reliable calculation tools, which may bring benefit to the efficiency of designing the HTHEs, are not numerous. The widely used lumped methods, such as logarithmic mean temperature difference (LMTD) and the number of transfer units (NTU) method, are applicable thereto. Both methods, in general, require inlet and outlet temperatures of the fluids, though they may involve the iteration procedure when the outlet temperatures are to be determined [15]. Schulte-Fischedick *et al.* [16] made use of the LMTD method in designing a prototype ceramic HTHE for an externally fired combined cycle of 6 MWel output fueled with woody biomass. The plate-fin flue gas/air heat exchanger was designed as a counter-flow type. Baina *et al.* [17] utilized the NTU method to model two types of exhaust gas/air HTHEs, the corrugated plate one and of shell-and-tube type, for the EFGT system fueled with biomass producer gas. The reported discrepancies between the experimental data and predictions for a plate heat exchanger in terms of outlet temperatures of working air and flue gas did not exceed 1.5% and 2.1%, respectively. The same calculation method was applied by Al-attab and Zainal [18] to determine the heat exchange surface area of a stainless steel HTHE designed for a small-scale EFGT system fired

with waste wood blocks (of $\sim$ 57 kWth and $\sim$ 5.6 kWel). A more advanced approach was applied by Jolly *et al.* [19], who developed a numerical code to determine the heat transfer and pressure drop characteristics and optimize the initial design concept of a bayonet tube gas-gas HTHE. The program utilized the semi-explicit method, wherein the problem was reduced to one-dimensional (1D) calculations solving basic equations for a modular unit of a designed heat exchanger. The model also involved the radiation between the flue gas and the tube surface. Cordiner and Mulone [2] proposed a 1D thermal balance approach with a two-zone combustion model to account for the heat release and radiation contribution and simulated the performance of biomass furnace-integrated HTHE in the micro-EFGT system of $\sim$ 70 kW electric power output.

As the literature review shows, the relatively simple and computationally efficient approaches for developing the HTHEs designs for micro-scale CHP units are rather limited. The objective of the present work is to demonstrate the in-house numerical approach that served as a support in designing a red-hot air furnace for a small-scale EFGT system, whilst taking account of the specific technological and technical limits. Despite the unique design concept of the furnace under consideration, to evaluate the heat transfer between the hot side stream (flue gas) and tube side stream (working air), the basic governing equations, including the correlations for conduction, convection and radiation, were utilized in the computational solution method. Focusing on the design simplicity, computer code flexibility, and optimization usability, the calculation procedure makes use of iteration methods and multiplication of predefined tubing sub-elements (tube segments) of the heat exchange sections. The developed simulation tool was used for multivariant analysis to find the optimum, in terms of heat transfer rate and manufacturing costs, furnace design for the defined inlet thermal and flow parameters. This eventually allowed to determine the required heat exchange surface area of the furnace. The computation results were then validated through the experimental study of a designed laboratory-scale air furnace.

2 The furnace design assumptions

The general aim that lies behind the development of the calculation methodology presented herein was to draw up the basic design guidelines for the small-scale red-hot air furnace (RHAF) of 20 kW capacity, performing the

role of a heat source in a CHP unit using an externally-fired gas turbine. The RHAF is intended to heat the working air to the designed temperature exceeding 800°C under low-pressure flow conditions [1]. Given the techno-economical limits, resulting from the high-temperature operational regimes of a device to be involved and, on the other hand, from the thermal and mechanical properties of materials available on the market, a two-module design of a furnace was assumed.

The furnace is considered to be composed of high-temperature (HT) and medium-temperature (MT) sections. The HT part (the red-hot section) is modeled as a two-zone section, wherein the first is a firebox and the other is the remaining part of a combustion chamber with the wall tubes. The MT part is limited to the heat exchange section separated from the direct fire zone and involves convection as the dominating heat transfer mechanism. This concept is intended to reduce the use of costly heat-resistant materials. Thus, the austenitic heat-resistant steel (AISI 304) was taken into consideration only for the HT section, and the first zone of the MT part. The maximum permissible long-term operation temperature for this type of steel is approximately 1150°C. The convection part of the heat exchanger is made of P265GH boiler steel. The screening tubes in the HT section were assumed to consist of bent parallel tubes for each wall of the combustion chamber (Fig. 1a). The MT heat exchange part constitutes the flue gas channel with the bundle of parallel tubes, bent in the horizontal plane as demonstrated in Fig. 1b. The furnace is assumed to be fired by propane (C_3H_8).

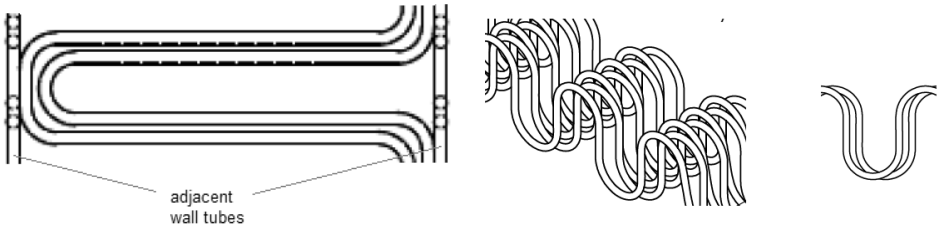

(a) (b)

Figure 1: The geometry of furnace tubing sub-elements: a) wall tubing segment in the high-temperature section; b) tube bundle in the medium-temperature section, the spatial view (left) and the side view on the tube bundle segment (right).

3 Calculation details

The calculation code was developed to determine the required heat exchange surface for the target outlet temperature of the working air, based on the set input thermal and flow parameters on the hot and cold sides, which included:

- the amount and temperature of combustion air;
- the temperature of working air at the furnace inlet and outlet, and the outlet from the MT section; the latter is assumed at the level of the maximum temperature permissible for the boiler steel.

For simplicity, the counter-current flow of media, i.e. the working fluid (air) and flue gas, is considered.

The required heat exchange surface is expressed as

$$A = \frac{\dot{Q}}{k\theta}\,, \tag{1}$$

where $\dot{Q}$ is the thermal output, k represents the overall heat transfer coefficient given as

$$k = \frac{1}{\alpha_{fg}} + \frac{\delta}{\lambda_w} + \frac{1}{\alpha_a} \tag{2}$$

with α_{fg} and α_a denoting the heat transfer coefficient on the hot and cool sides, respectively. The parameters δ and λ_w stand for the thickness and thermal conductivity of a tube wall, respectively. The heat transfer coefficient for the hot side (flue gas) takes into account both, the convection and radiation heat transfer coefficients, and is given as

$$\alpha_{fg} = \alpha_{fg}^{\mathrm{conv}} + \alpha_{fg}^{\mathrm{rad}}\,. \tag{3}$$

The parameter θ is the mean logarithmic temperature difference, defined as follows:

$$\theta = \frac{\Delta T_1 - \Delta T_2}{\ln \dfrac{\Delta T_1}{\Delta T_2}}\,, \tag{4}$$

where

$$\Delta T_1 = T_{fg}^{\mathrm{in}} - T_a^{\mathrm{out}} \quad \textit{and} \quad \Delta T_2 = T_{fg}^{\mathrm{out}} - T_a^{\mathrm{in}}\,.$$

In the above, T denotes temperature, and superscripts in and out refer to the inlet and outlet parameters of the hot and cold fluids, flue gas (subscript fg) and working air (subscript a), respectively.

3.1 Radiation on the flue-gas side

The triatomic components of flue gas, i.e. water and carbon dioxide (H_2O and CO_2), are accounted for in the calculation of radiation heat transfer. Since the burning of gaseous fuel (propane) was considered, no additional thermal radiation from the particulate matter was included in the analysis. The radiation heat transfer coefficient between the flowing gas (g) and the surface (s) is expressed by the formula [20]

$$\alpha_{\mathrm{rad}} = \frac{\dot{q}}{T_s - T_g} = \frac{\varepsilon_s + 1}{2}\sigma\varepsilon T_g^3 \frac{1 - \left(\frac{T_s}{T_g}\right)^4}{1 - \left(\frac{T_s}{T_g}\right)}, \tag{5}$$

where $\dot{q}$ represents the density of heat flux, σ is a Stefan-Boltzmann constant, and ε is the thermal emissivity, whereby the latter without index refers to the radiating medium in the combustion chamber (including luminous and non-luminous part), and the other with superscript s refers to the irradiated surface.

As regards the HT heat exchange section, its emissivity may be calculated from

$$\varepsilon = \frac{\varepsilon_{fl}}{\varepsilon_{fl} + (1 - \varepsilon_{fl})\,\psi\xi}, \tag{6}$$

where ψ is the degree of wall screening, and ξ is the slagging factor. The latter, for gaseous fuels, amounts to 0.8 [20]. Parameter ε_{fl} refers to the flame emissivity that depends on the emissivity of the luminous part of the flame (ε_l) related to the glowing particulates (ash and soot), and that of the gaseous non-luminous part (ε_g)

$$\varepsilon_{fl} = m\varepsilon_l + (1 - m)\varepsilon_g, \tag{7}$$

where m represents the flame-to-chamber volume ratio, which for the case of gaseous fuel burning is assumed at 0.2 [20]. Emissivity ε_l is given as

$$\varepsilon_l = 0.9\left[1 - \exp\left(-k_p pL\right)\right], \tag{8}$$

where p denotes pressure in the firebox, and k_p is a temperature-dependent absorption coefficient described by

$$k_p = 1.6\frac{T}{1000} - 0.5. \tag{9}$$

Parameter $L = 3.6\dfrac{V}{F}$ stands for the thickness of the radiating gas layer as the ratio of the volume of a combustion chamber (V) and the total irradiated surface (F).

In the case studied the surface F is the sum of the chamber walls and the screening tubes' outer surface. The emissivity of the non-luminous part, i.e. the flue gas, is expressed by

$$\varepsilon_g = 1 - \exp\left(-k_g L\right), \tag{10}$$

where k_g is the absorption coefficient given as [20]

$$k_g = \frac{0.8 + 1.6 X_{H_2O}}{\sqrt{p_n L}} \left(1 - 0.38 \frac{T}{1000}\right) \left(X_{\mathrm{H_2O}} + X_{\mathrm{CO_2}}\right). \tag{11}$$

In the above, $X_{\mathrm{H_2O}}$ and $X_{\mathrm{CO_2}}$ represent the mole fractions of water and carbon dioxide, respectively, and p_n denotes the partial pressure of these components.

Further, to describe the degree of wall screening (ψ), the ratio of the tubes' surface (A_s) to the chamber wall surface (A_w), i.e. $\psi = A_s/A_w$ was adopted [20]. In the MT heat exchange section, the non-luminous gas layer is considered. In this case, parameter m (Eq. (7)) amounts to 0, which implies $\varepsilon = \varepsilon_g$ in Eq. (5).

3.2 Convection heat transfer

Knowing the Nusselt number (Nu), the heat transfer coefficient may be calculated as

$$\alpha = \frac{\mathrm{Nu}\,\lambda_f}{L}, \tag{12}$$

where λ_f represents the thermal conductivity of the fluid and is determined using the correlation [21, 22]

$$\mathrm{Nu} = C\mathrm{Re}^n\mathrm{Pr}^m, \tag{13}$$

where the constants C, n, and m depend on the character of the flow (laminar, transition, turbulent) [21,22]. For the cold side, the characteristic dimension L is the inner diameter, $L = d_{\mathrm{inn}}$, and for the hot side (flue gas flow), this dimension is represented by the hydraulic diameter.

3.3 Fuel combustion

Following the assumed limit for the tube wall temperature in the firebox ($< 1150°C$), the combustion with an excess of air was considered. Taking into account the heat loss to the surroundings ($\dot{Q}_{\text{loss}}$), the energy balance for the combustion chamber takes the form

$$\dot{H}_{ox}^{\text{in}} + \dot{H}_{f}^{\text{in}} + \dot{Q}_{\text{LHV}} = \dot{H}_{fg} + \dot{Q}_{\text{loss}}\,, \tag{14}$$

where $\dot{H}$ represents the mass flow enthalpy and $\dot{Q}_{\text{LHV}}$ stands for the fuel chemical energy.

For a set flue gas temperature at the outlet from the furnace to the chimney (T_{fg}^{out}), the heat given off by the hot medium is expressed as

$$\dot{Q}_{fg} = \dot{m}_{fg}\bar{c}_{p,fg}\left(T_{\text{com}} - T_{fg}^{\text{out}}\right) \tag{15}$$

and the heat absorbed by the working air is determined from

$$\dot{Q}_{a} = \dot{m}_{a}\bar{c}_{p,a}\left(T_{a}^{\text{out}} - T_{a}^{\text{in}}\right). \tag{16}$$

Parameter T_{com} in Eq. (15) represents theoretically calculated combustion temperature, whereas $\bar{c}_p$ refers to the specific heat of respective fluids for arithmetically averaged temperature between the inlet and outlet values. The details for the physicochemical properties of fuel and fluids are provided elsewhere [1].

3.4 Numerical procedure

The calculations for each heat exchange section of a furnace, i.e. the HT and MT sections, are carried out in separate loops, starting from determining the parameters in the firebox. The flow diagram of a numerical algorithm is shown in Figs. 2 and 3. The calculation procedure involves the following steps:

i. Given the temperatures and mass flow rates of combustion air and fuel, the combustion temperature is determined (using Eq. (14)). Owing to the dependence of the flue gas heat capacity on temperature, the iterative method is utilized. The initial temperature, which is the calculated adiabatic combustion temperature of C_3H_8(T_{ad}), is decreased by $dT = 0.1$ K in each step until the convergence between

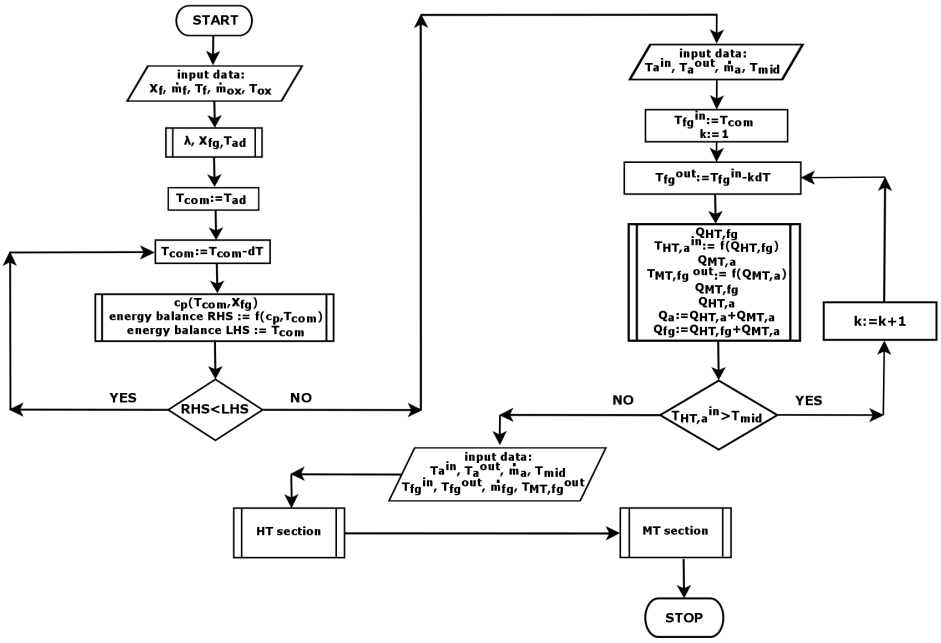

Figure 2: The general flow diagram of the developed numerical algorithm for designing the furnace.

the left-hand (LHS) and right-hand sides (RHS) of the equation is reached. The resulting temperature value (T_{com}) is the inlet temperature of the HT heat exchange section of a furnace.

ii. For the input parameters of working air (i.e. flow rate ($\dot{m}_a$), temperatures at the inlet to (T_a^{in}), and the outlet from the furnace (T_a^{out}), and additionally in between the MT and HT sections), and given T_{com}, the flue gas outlet temperature (T_{fg}^{out}) is calculated based on the flue gas/working air energy balance. This is done by iteratively decreasing the flue gas temperature leaving the HT section until the assumed air temperature between the MT and HT sections (T_{mid}) is achieved for a set convergence criterion. The energy balance for the HT section is calculated for the determined inlet and outlet temperatures of the fluids in the section.

iii. The results of the iterative temperature calculations are the input data to the design loops of the HT and MT sections.

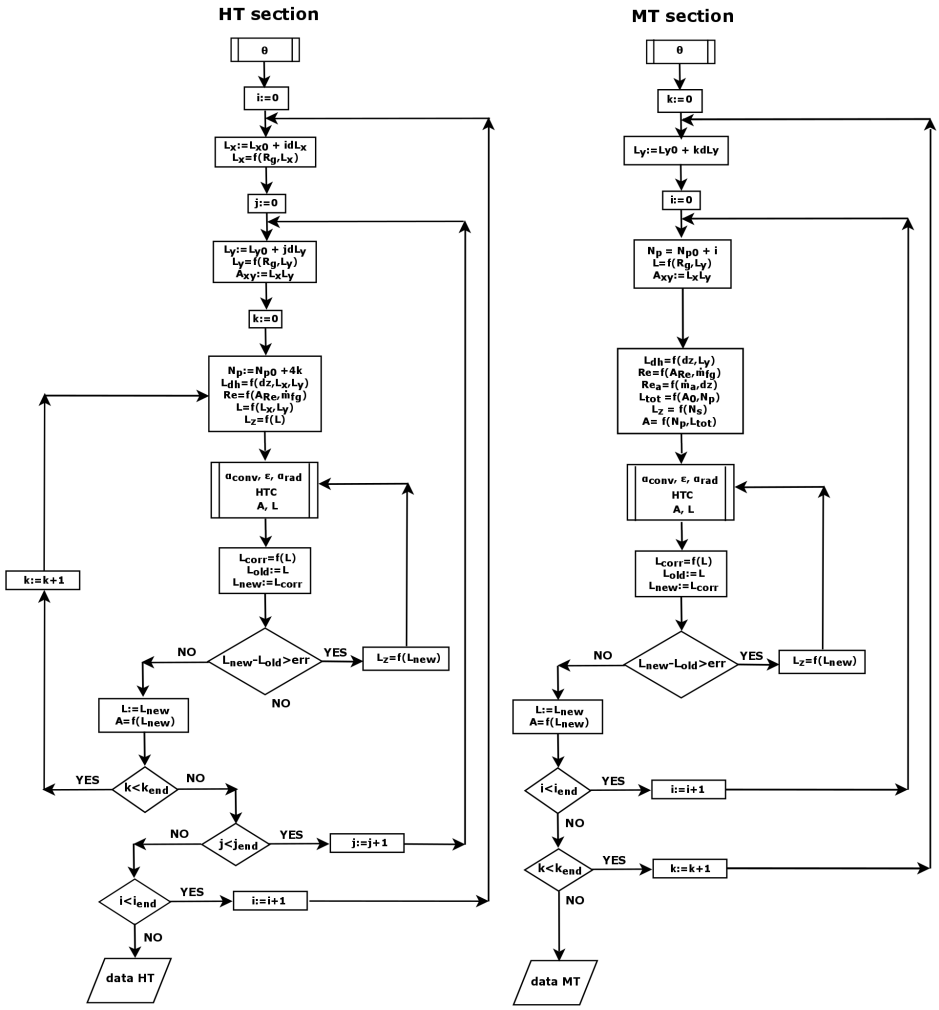

Figure 3: Detailed schemes of numerical algorithms for calculations in HT and LT sections of a furnace.

iv. The mean logarithmic temperature difference θ (Eq. (4)) in the HT section is calculated.

v. Starting from the initial geometry (L_{x0}, L_{y0}) of the section and based on the technical parameters related to tube bending (L – the length of the flue channel, R_g – bending diameter, and wall tubing configuration), the geometry of the firebox with the integrated HT heat exchange section is presumed by multiplying the tubing segments.

vi. For the set geometry, the flow characteristics (Re and Nu numbers, heat transfer coefficients) are determined to calculate the total heat transfer coefficient (k) in the HTC procedure and, eventually, the required heat exchange surface area (A) using Eq. (1).

vii. Steps (iv)–(vi) are then executed for the MT section while accounting for the assumed shape and arrangement of bent tubes in the flue gas channel.

4 Model predictions and experimental validation

The developed methodology allowed for the parametric analysis of the thermal characteristics of the design to aid the choice of an optimum solution in terms of required outlet temperatures and construction cost. The key variable geometrical parameters involved the dimensions of the combustion chamber and flue gas channel, and the number of tubes. The convection part of the furnace (MT) can be analyzed separately from the HT part, however, due to technical reasons the geometry of the screening tubes implies the number of tubes in the bundle in the MT section. Also, due to practical reasons, of importance was the total length of a single tube in each section, either in the HT or the MT section, which is related to the standard tube lengths available on the market. The results of a numerical parametric analysis are shown in Figs. 4 and 5. The input data were chosen as the main assumptions for designing the whole system, which were: the

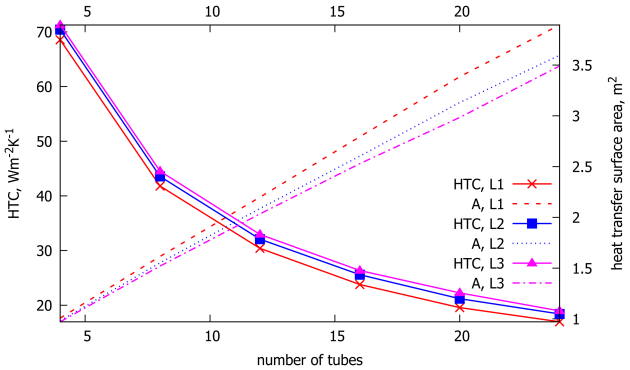

Figure 4: Heat transfer coefficient (HTC) and heat transfer area (A) in the HT heat exchanger section *vs.* the number of tubes for different cross-sections of a combustion chamber: $L1 = 0.5 \cdot 0.5$ m^2, $L2 = 0.75 \cdot 0.75$ m^2, $L3 = 1 \cdot 1$ m^2.

mass flow rates for the flue gas and the working air, the input fluid temperatures, the required output temperature for working air and its temperature between the HT and MT sections ($T_{\mathrm{mid}} = 624°\mathrm{C}$). Due to the available sizes of the steel and heat-resistant boiler tubes and the need to connect them between the MT and HT sections, only one diameter size (outer diameter of $21.3 \cdot 10^{-3}$ m) was taken into consideration. Additionally, because of the technical limit on the tube bending radius, the minimum values of the radius for the HT and MT sections were accounted for, i.e. $93.15 \cdot 10^{-3}$ m and $77.5 \cdot 10^{-3}$ m, respectively. The input data for the fuel flow rate results from the required thermal power output of the furnace. In addition, heat losses to the surroundings at 15% of the total chemical fuel energy were assumed.

The correlation between the overall heat transfer coefficient (HTC) and the number of tubes in the radiative (HT) section is presented in Fig. 4. As it can be seen, the HTC value is higher for a lower number of tubes, which then results from higher Re values for the flow of working air. In other words, the more tubes the slower the airflow and the lower HTC. Correspondingly, for a smaller number of tubes, as expected, the total heat transfer surface area needed to achieve the set operation parameters is smaller. Moreover, the smaller size (cross-sectional area) of a combustion chamber translates into a higher value of overall HTC, which is due to higher Re for flue gas flow in a smaller cross-section area.

A similar trend may be observed in the case of a correlation between the overall HTC and the number of tubes in the convective (MT) section. As it can be seen from Fig. 5, the HTC value is higher for a lower number

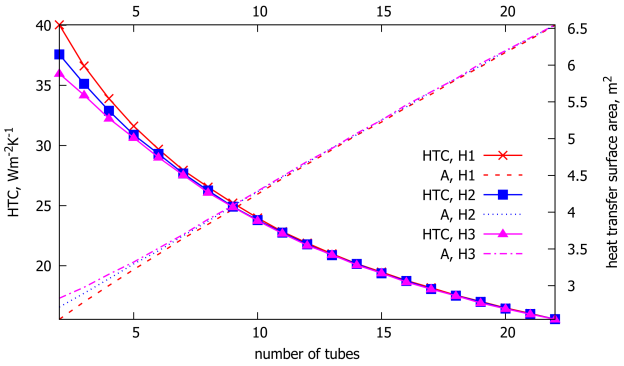

Figure 5: Heat transfer coefficient (HTC) and heat transfer area (A) in the MT heat exchanger section *vs.* the number of tubes for different heights of the flue gas channel: $H1 = 0.35$ m, $H2 = 0.5$ m, $H3 = 0.65$ m.

of tubes (again, it results from increased Re of the airflow for a decreasing number of tubes). Consequently, the predicted heat transfer area is smaller for a lower number of tubes. Moreover, an increase in the height of a flue gas channel results in lowering overall HTC, which comes from the lower Re value for flue gases in the greater cross-section area. It should be noted that in the proposed calculation methodology, the width of the flue gas channel is defined by the number of tubes. The influence of the channel height on the HTC and heat transfer area is visible only for the number of tubes lower than 10, which stems from the flow laminarisation effect in the case of a greater number of tubes.

Comparing Figs. 4 and 5 one may see that the maximum value of overall HTC for the HT section is nearly twice as high as that for the MT section (e.g. 70 W/m^{2}K *vs.* 40 W/m^{2}K), which is due to additional radiative effects in a combustion chamber. The heat transfer surface area predicted for this section is thus almost twice as small as that for the MT section (4 m^2 *vs.* 6.5 m^2).

The calculation results of the selected design variant, including basic thermal and flow parameters, and main dimensions of both furnace heat exchange sections, are presented in Table 1. As aforementioned, greater

Table 1: Parametric characteristics of a furnace – sample calculation results.

MT heat exchange section							
Number of tubes	Channel width (m)	Re_{fg}	Re_a	k (W/(m^{2}K))	A (m^2)	$\dot{Q}$ (kW)	Section length* (m)
6	0.28	1069	8093	29.7	3.4	15.0	0.7
8	0.36	832	6070	26.5	3.8		0.6
10	0.45	680	4856	24.0	4.3		0.5
16	0.70	440	3035	18.8	5.4		0.4
HT heat exchange section							
Number of wall tubes	Section cross-area (m^2)	Re_{fg}	Re_a	k (W/(m^{2}K))	A (m^2)	$\dot{Q}$ (kW)	Section height (m)
8	$0.4 \cdot 0.4$	939	4374	40.5	1.7	8.7	2.5
16	$0.4 \cdot 0.4$	751	2187	22.7	2.9		2.5
8	$0.5 \cdot 0.5$	791	4374	41.8	1.6		2.1
16	$0.5 \cdot 0.5$	653	2187	23.8	2.8		2.1

*) for three-pass flue gas channel flow assumed

tube number in both sections contributes to lowering cold and hot fluid flow parameters, which leads to a decrease in the overall HTC and thereby to increased needed heat transfer area. Considering the technical limitations and possible pressure drop increase, eight tubes were taken for the design. The designed air furnace has undergone the experimental test series to validate the calculation outcomes [1]. The measurement results and predicted parameters are in satisfactory agreement, as shown in Table 2 (in the table, input values for calculation are marked in bold). As can be seen, the relative difference between the experimentally obtained and calculated outlet temperature of heated working air is only 2.7%, whereas in the case of outlet parameters on the hot side (flue gas) these differences do not exceed 5%.

Table 2: Comparison of simulation/predicted and measured parameters.

Parameter	Calculation	Measurements [1]	Relative difference, %
Fuel mass flowrate ($\dot{m}_f$), kg/h	**3.07**	3.14	2.2
Combustion air flowrate ($\dot{m}_{ox}$), kg/h	**80.0**	87.0	8.0
Flue gas flowrate ($\dot{m}_{fg}$), kg/h	83.07	90.14	7.8
Working air flowrate ($\dot{m}_a$), kg/h	**89.0**	83.3	6.8
Fuel temperature (T_f), °C	**20**	20	–
Combustion air temperature (T_{ox}), °C	**20**	35	–
Outlet flue gas temperature (T_{fg}^{out}), °C	206	215	4.2
Inlet working air temperature (T_a^{in}), °C	**46**	52	–
Outlet working air temperature (T_a^{out}), °C	926	951	2.6

5 Summary

In this paper, the approach developed to design the red-hot air furnace for the small-scale combined heat and power systems based on the externally-fired gas turbines was presented. The calculation procedure implemented in the in-house numerical code to predict the furnace performance, based on the required output thermal parameters, as well as on the material-related and manufacturing technical limitations, was demonstrated. The developed computational program has served to determine the heat exchange surface area of an optimized, in terms of heat transfer rate and manufacturing costs, design of the furnace.

The proposed algorithm enables the determination of the main geometrical parameters of both, high- and medium-temperature sections of the furnace. It was shown that using more tubes in both sections leads to lower cold and hot fluid flow parameters, and in consequence, to lower overall heat transfer coefficients and larger required heat transfer area. The latter affects the device size and its manufacturing cost. Taking into account the economic aspect, the obtained data enables choosing the optimal geometrical parameters for the construction of the red-hot air furnace while minimizing its cost at the same time.

The developed code allows for a multivariant analysis of the furnace designs and has resulted in the construction of the device that achieved the target operational parameters. Thereby, the approach used proved itself to be reliable in designing and optimizing effective high-temperature air furnaces and showed its usefulness in the future development of such devices.

Acknowledgements

The study was financially supported by the National Centre for Research and Development within the framework of the project VoltAeris (Project No. POIR.04.01.04-00-014/17).

Received 30 November 2023

References

[1] Kardaś D., Polesek-Karczewska S., Turzyński T., Wardach-Święcicka, Hercel P., Szymborski J., Heda Ł.: *Thermal performance enhancement of a red-hot air furnace for a micro-scale externally fired gas turbine system.* Energy **282**(2023), 128591.

[2] Cordiner S., Mulone S.: *Experimental-numerical analysis of a biomass fueled microgeneration power-plant based on microturbine.* Appl. Therm. Eng. **71**(2014), 905–912.

[3] Kobyłecki R., Zarzycki R., Bis Z., Panowski M., Wiński M.: *Numerical analysis of the combustion of straw and wood in a stoker boiler with vibrating grate.* Energy **222**(2021), 119948.

[4] Al-Attab K.A., Zainal Z.A.: *Externally fired gas turbine technology: a review.* Appl. Energ. **138**(2015), 474–487.

[5] Pantaleo A.M., Camporeale S.M., Shah N.: *Thermo-economic assessment of externally fired micro-gas turbine fired by natural gas and biomass: applications in Italy.* Energ. Convers. Manage. **75**(2013), 202–213.

[6] Bdour M., Al-Addous M., Michael Nelles M., Ortwein A.: *Determination of optimized parameters for the flexible operation of a biomass-fueled, microscale externally fired gas turbine (EFGT).* Energies **9**(2016), 856.

[7] Chai L., Tassou S.A.: *A review of airside heat transfer augmentation with vortex generators on heat transfer surface.* Energies **11**(2018), 2737.

[8] Rutkowski Ł., Szczygieł I.: *Calculation of the furnace exit gas temperature of stoker fired boilers.* Arch. Thermodyn. **42**(2021), 3, 3–24.

[9] Aziz A., Rehman S.: *Analysis of non-equidistant baffle spacing in a small shell and tube heat exchanger.* Arch. Thermodyn. **41**(2020), 2, 201–221.

[10] Hanuszkiewicz-Drapała M., Bury T., Widziewicz K.: *Analysis of radiative heat transfer impact in cross-flow tube and fin heat exchangers.* Arch. Thermodyn. **37**(2016), 1, 99–112.

[11] Kontogeorgos D.A., Keramida E.P., Founti M.A.: *Assessment of simplified thermal radiation models for engineering calculations in natural gas-fired furnace.* Int. J. Heat Mass Transf. **50**(2007), 5260–5268.

[12] Żukowski W., Migas P., Gwadera M., Larwa B., Kandafer S.: *A numerical analysis of heat transfer in a cross-current heat exchanger with controlled and newly designed air flows.* Open Chem. **16**(2018), 627–636.

[13] Thek G., Brunner T., Oberberger I.: *Externally with biomass and internally with natural gas fired micro gas-turbine-system, furnace and high temperature heat exchanger design as well as performance data from first test runs.* In: Proc. 18th Eur. Biomass Conf. Exhib., Lyon 2010, 1891–1899.

[14] Wajs J., Kura T., Mikielewicz D., Fornalik-Wajs E., Mikielewicz J.: *Numerical analysis of high temperature minichannel heat exchanger for recuperative microturbine system.* Energy **238**(2022), 121683.

[15] Kardaś D., Wardach-Święcicka I., Grajewski A.: *Partially transient one-dimensional thermal-flow model of a heat exchanger, upwind numerical solution method and experimental verification.* Arch. Thermodyn. **43**(2022), 4, 63–83.

[16] Schulte-Fischedick J., Dreißigacker V., Tamme R.: *An innovative ceramic high temperature plate-fin heat exchanger for efcc processes.* Appl. Therm. Eng. **27**(2007), 1285–1294.

[17] Baina F., Malmquist A., Alejo L., Palm B., Fransson T.H.: *Analysis of a high-temperature heat exchanger for an externally-fired micro gas turbine.* Appl. Therm. Eng. **75**(2015), 410–420.

[18] Al-Attab K.A., Zainal Z.A.: *Performance of high-temperature heat exchangers in biomass fuel powered externally fired gas turbine systems.* Renew. Energy **35**(2010), 913–920.

[19] Jolly A.J., O'Doherty T., Bates C.J.: *COHEX: A computer model for solving the thermal energy exchange in an ultra high temperature heat exchanger. Part A: Computational theory.* Appl. Therm. Eng. **18**(1998), 1263–1276.

[20] Orłowski P.: *Steam boilers – design and calculation.* WNT 1972, Warszawa (in Polish).

[21] Hobler T.: *Heat transfer and heat exchangerS.* WNT 1986, Warszawa (in Polish).

[22] Serth R.W., Lestina T.G.: *Process heat transfer. Principles, applications and rules of thumb* (2nd edn.). Academic Press, 2014.